63-2-3

Monthly Progress Report P-B1881-8

DEVELOPMENT OF BROAD-BAND ELECTROMAGNETIC ABSORBERS FOR ELECTRO-EXPLOSIVE DEVICES

by

Paul F. Mohrbach
Robert F. Wood

November 1, 1962 to November 30, 1962

Prepared for

U.S. NAVAL WEAPONS LABORATORY
Dahlgren, Virginia
Code DDR

N178 - 8887

THE FRANKLIN INSTITUTE
LABORATORIES FOR RESEARCH AND DEVELOPMENT
PHILADELPHIA PENNSYLVANIA

THE FRANKLIN INSTITUTE • *Laboratories for Research and Development*

Monthly Progress Report

P-B1981-5

DEVELOPMENT OF BROAD-BAND ELECTROMAGNETIC ABSORBERS FOR ELECTRO-EXPLOSIVE DEVICES

by

Paul F. Mohrbach
Robert F. Wood

November 1, 1962 to November 30, 1962

Prepared for

U.S. NAVAL WEAPONS LABORATORY
Dahlgren, Virginia
Code WMR

N178 - 8087

ABSTRACT

The effects upon attenuation of increasing conductivity is shown by substituting for ϵ'' its equivalent $\frac{\sigma}{2\pi f}$ in the general equation for attenuation. The equation indicates that attenuation should increase with conductivity if the other parameters are not adversely affected. A series of graphs of conductivity versus frequency for the theoretical models A-G is given.

A discussion of the effects of silvering toroids and the significant increase of attenuation resulting therefrom is given in table form. To eliminate effects of the silver, toroids were painted with an Aquadag solution on the inner and outer diameters. Attenuation values showed an increase but not to the same extent. This is probably because the Aquadag is not as conductive as the silver solution. It remains to be determined if all of the parameters are affected by silvering and to what extent.

The ferrous ion content is important in the fabrication of ferrites. A rapid cooling operation has been employed in the procedure and ferrites having over 35 db/cm at 500 Mc have been produced. The densities of our ferrites have been increased by using high firing temperatures.

Experiments were conducted to determine the effect of a ferrite RF attenuator on different types of firing stimuli. Oscillograms indicate that neither capacitor discharge pulses nor constant current pulses are altered by the ferrite attenuator.

Our search for an RF attenuating material is not being limited to ferrites but are looking into other materials, such as organics. Literature has revealed that certain organics have a loss tangent greater than 1.0.

Evaluation of acryloid-bound barium titanate insulation was continued with a decrease in attenuation at 500 Mc of 20% for a three-mil coating. Voltage breakdown values ranged from 500-600 volts for the same coating.

A derivation of the terminating impedance corresponding to a maximum transfer of power through a section of transmission line is presented. The termination is defined in terms of the line characteristic impedance and propagation constant.

TABLE OF CONTENTS

LIST OF FIGURES

LIST OF TABLES

1. INTRODUCTION

The Franklin Institute, under contract to the Naval Weapons Laboratory and Picatinny Arsenal, has during the past several years been active in the search for materials which absorb or attenuate RF energy. A significant development has been the carbonyl iron attenuating material which provides adequate protection for frequencies above 100 Mc in a 1 cm length. However, as our knowledge of the problem increases, it appears that the most troublesome frequencies are below 10 Mc. Since we do not feel that the iron can be improved enough to be of avail in this range, it has become necessary to seek other materials for this purpose. The main scope of this study will comprise the investigation of new materials.

At the outset, our research indicated that the class of materials known as ferrites show promise, and particularly so if the dielectric and magnetic properties of these materials can be optimized. However, this study will not limit itself to any one type of material because other factors such as ease of manufacture and adaptability are also important and could narrow our choice.

Ultimately, it is planned to develop techniques and processes to use these materials in practical applications. This includes the application of a high-K dielectric to our attenuating material to improve its dc resistance and voltage breakdown properties.

A supporting instrumentation study and development program will run concurrently with the selection and development of any such material. Instrumentation developed to measure attenuation at the frequencies of concern (10 Mc and below) in itself will be advancing the state of the art. We are interested in true attenuation; not insertion loss. Since most of our samples are low impedance, this makes matching difficult, and matching is used in most of our attenuation measuring systems.

2. MATERIAL STUDY

2.1 Material Evaluation - Ferrites

Contributor: Daniel J. Mullen, Jr.

Materials are being sought which are effective in attenuating RF energy at low frequencies. The present study is concerned with evaluating ferrites of various types which are supplied by commercial ferrite manufacturers. On the basis of our evaluation, we expect to determine which type of ferrites show the most promise. This knowledge will be used to aid in the synthesis of material which represents the optimum in attenuation capacity.

2.1.1 Significance of Conductivity as a Criterion for Attenuation.

In last month's report, Tables 2-3 and 2-6 gave values of volume-resistivity for the theoretical models A through G. These values were not plotted in the graphs for reasons of simplicity. This month, a plot of the reciprocal of these values for all of the models will serve to illustrate how the conductivity varies with frequency. See Figures 2-1 through 2-7. In postulating a theoretical model to attain high attenuation, we purposely increased the values of ϵ', μ', $\tan \delta_\mu$ and $\tan \delta_\epsilon$. In so doing, it has been found that volume-resistivity should be low, or conversely, conductivity should be high. The following analysis should serve to demonstrate this.

It will be remembered that σ, dielectric conductivity in ohms/meter, is related to ϵ'', the lossy part of the complex permittivity by the expression:

$$\sigma = \omega\epsilon'' \quad \text{or} \quad \sigma = 2\pi f \epsilon''$$

If this relationship is substituted in our general expression for attenuation, it will be seen that increasing σ, has a direct bearing on increasing attenuation. This is shown as follows:

$$\alpha = 128 \times 10^{-11} f \left[k'_\epsilon k'_\mu \left((\tan \delta_\epsilon \tan \delta_\mu - 1) + \sqrt{1 + \tan^2\delta_\epsilon \tan^2\delta_\mu + \tan^2\delta_\epsilon + \tan^2\delta_\mu} \right) \right]^{\frac{1}{2}} \quad (2\text{-}1)$$

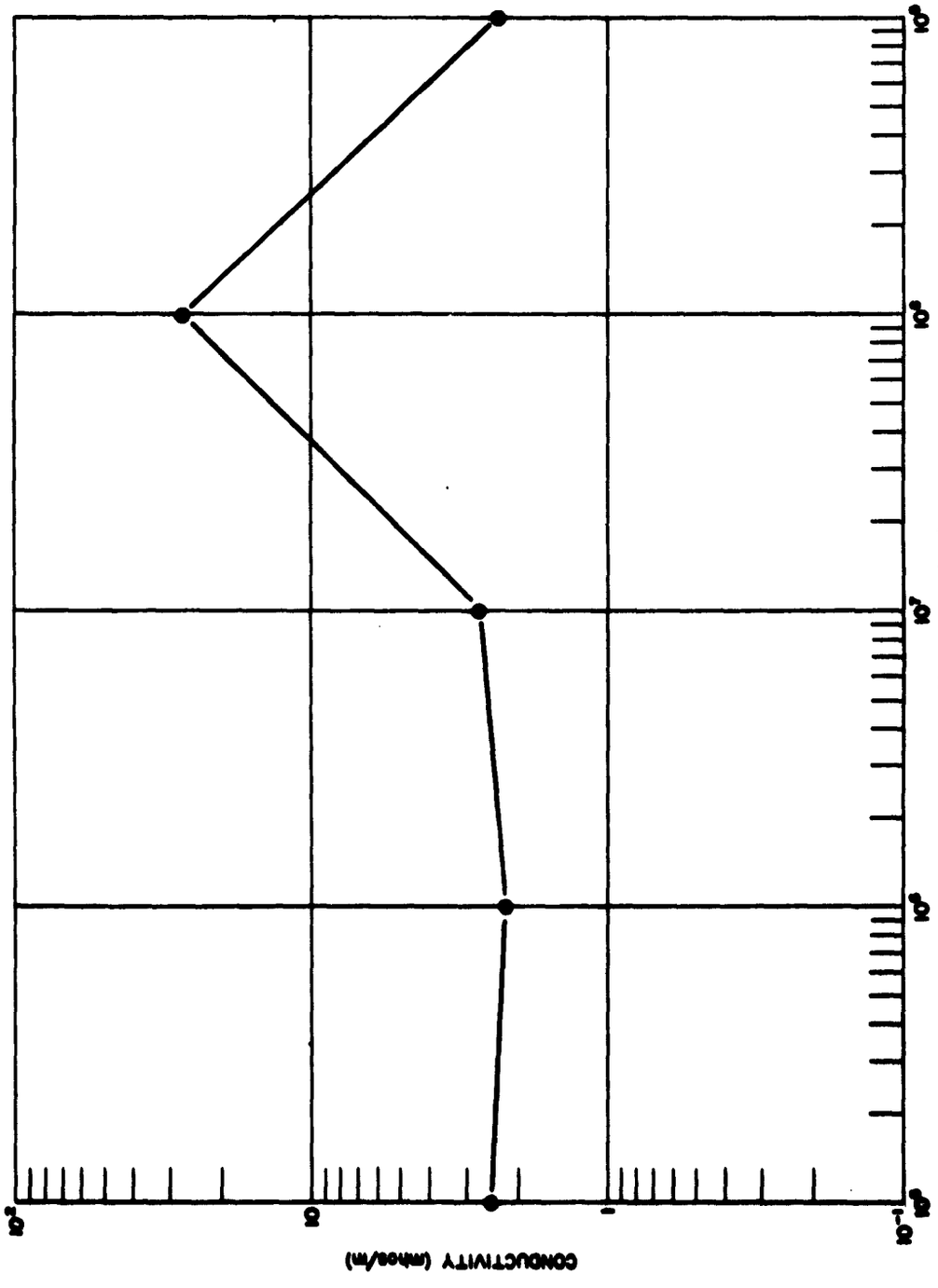

FIG. 2-1. CONDUCTIVITY VS. FREQUENCY FOR MODEL 4

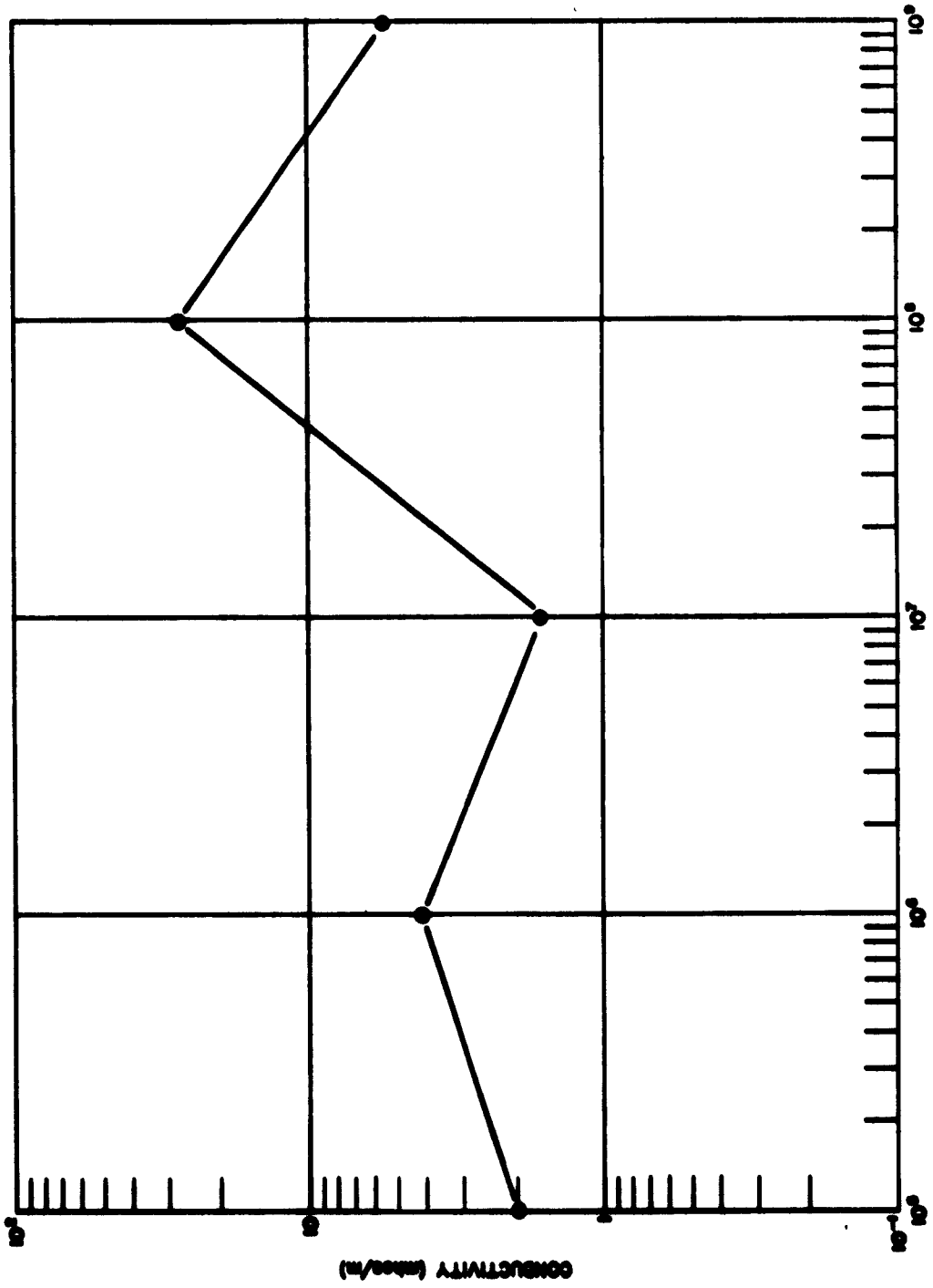

FIG. 2-2. CONDUCTIVITY VS. FREQUENCY FOR MODEL 8

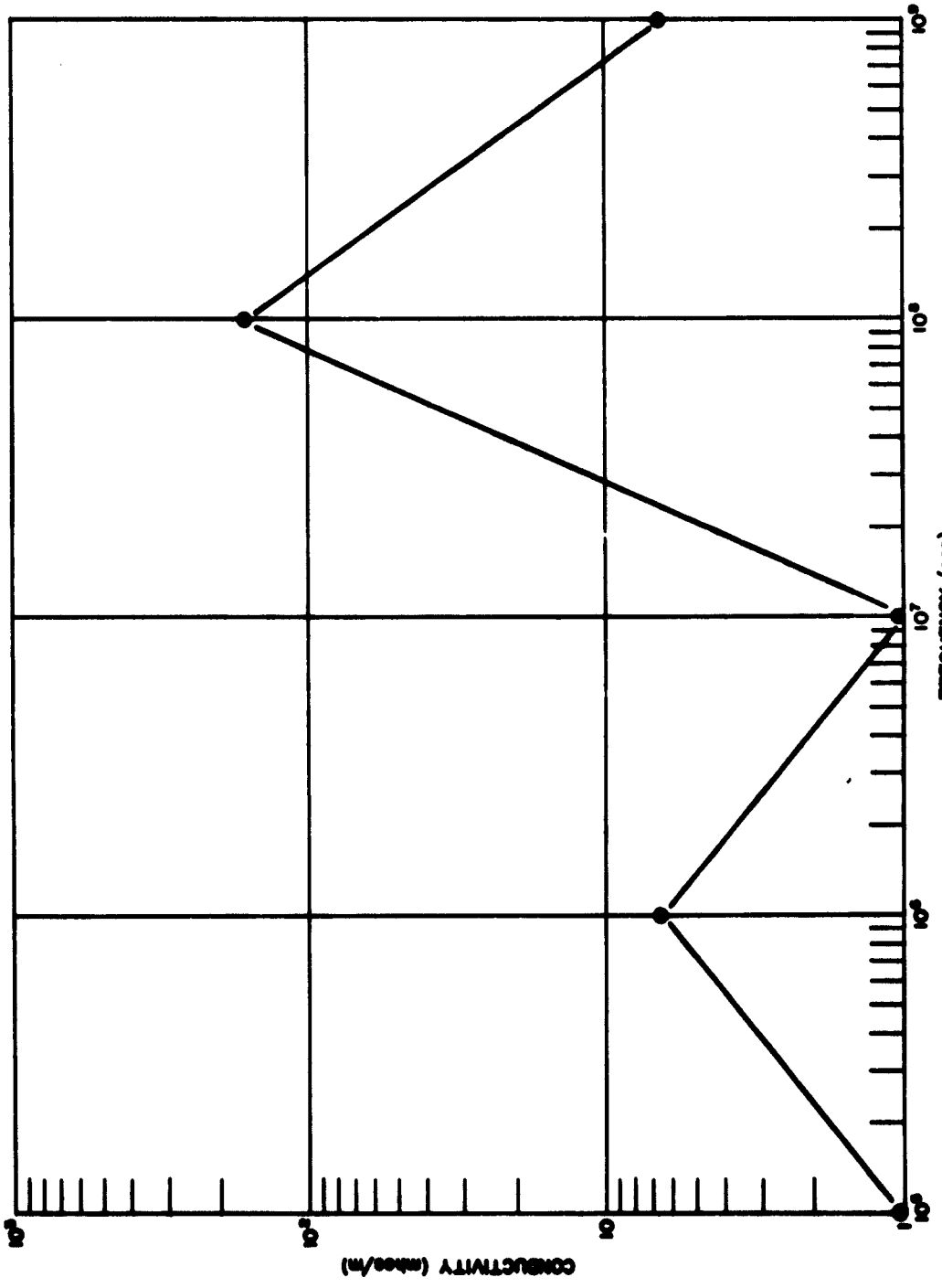

FIG. 2-3 CONDUCTIVITY VS. FREQUENCY FOR MODEL C

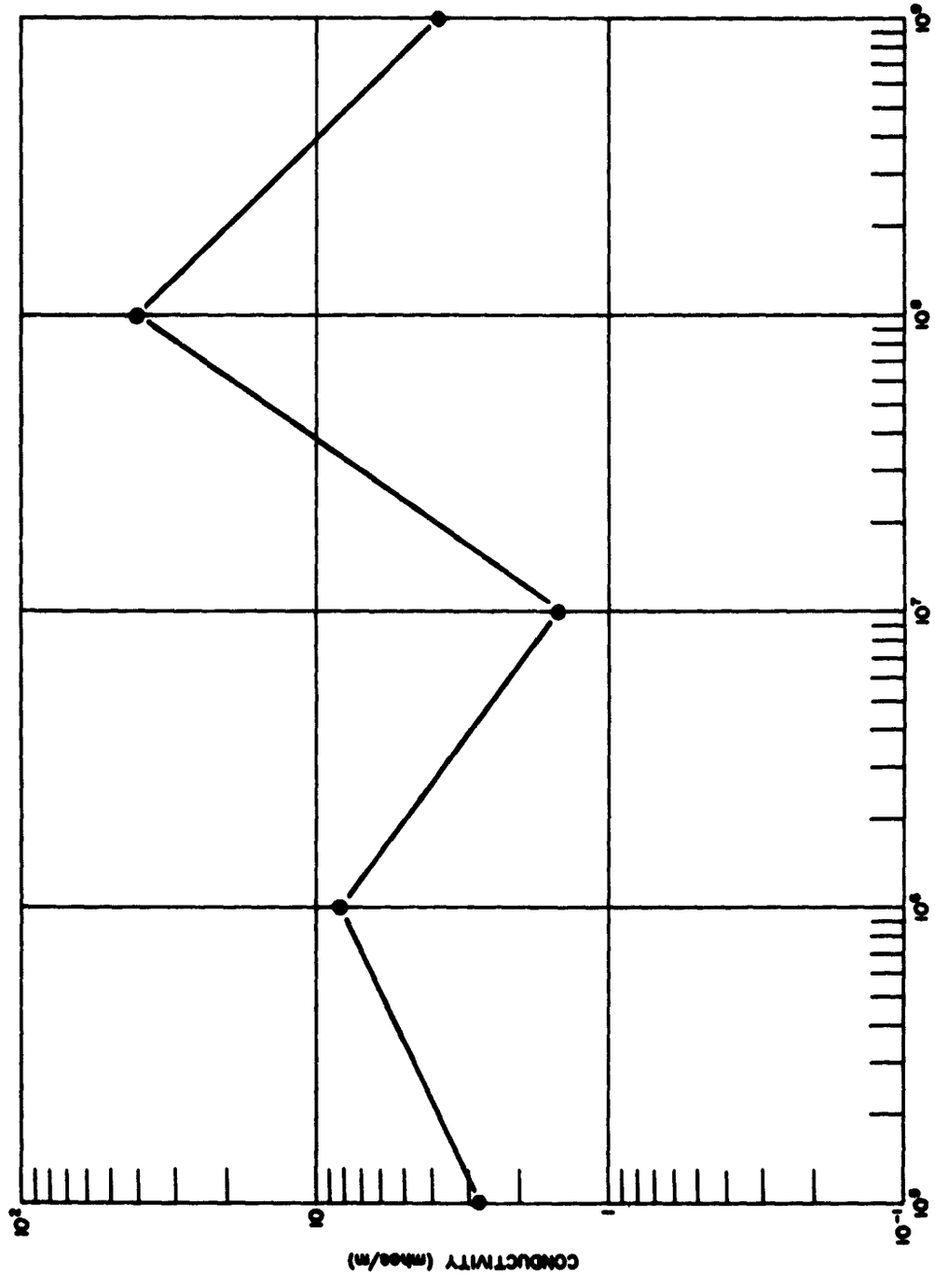

FIG. 2-4. CONDUCTIVITY VS. FREQUENCY FOR MODEL 0

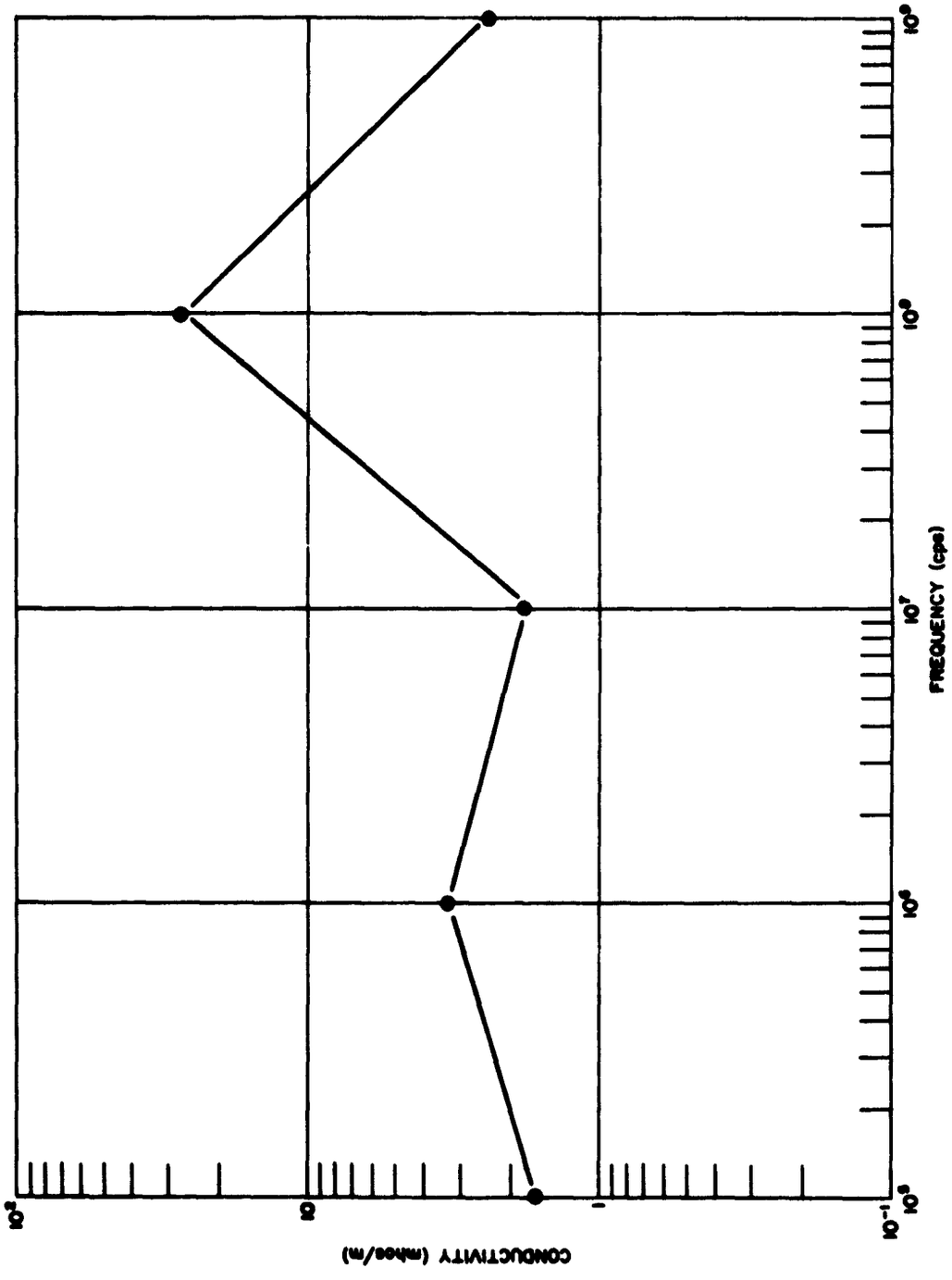

FIG. 2-5. CONDUCTIVITY VS. FREQUENCY FOR MODEL E

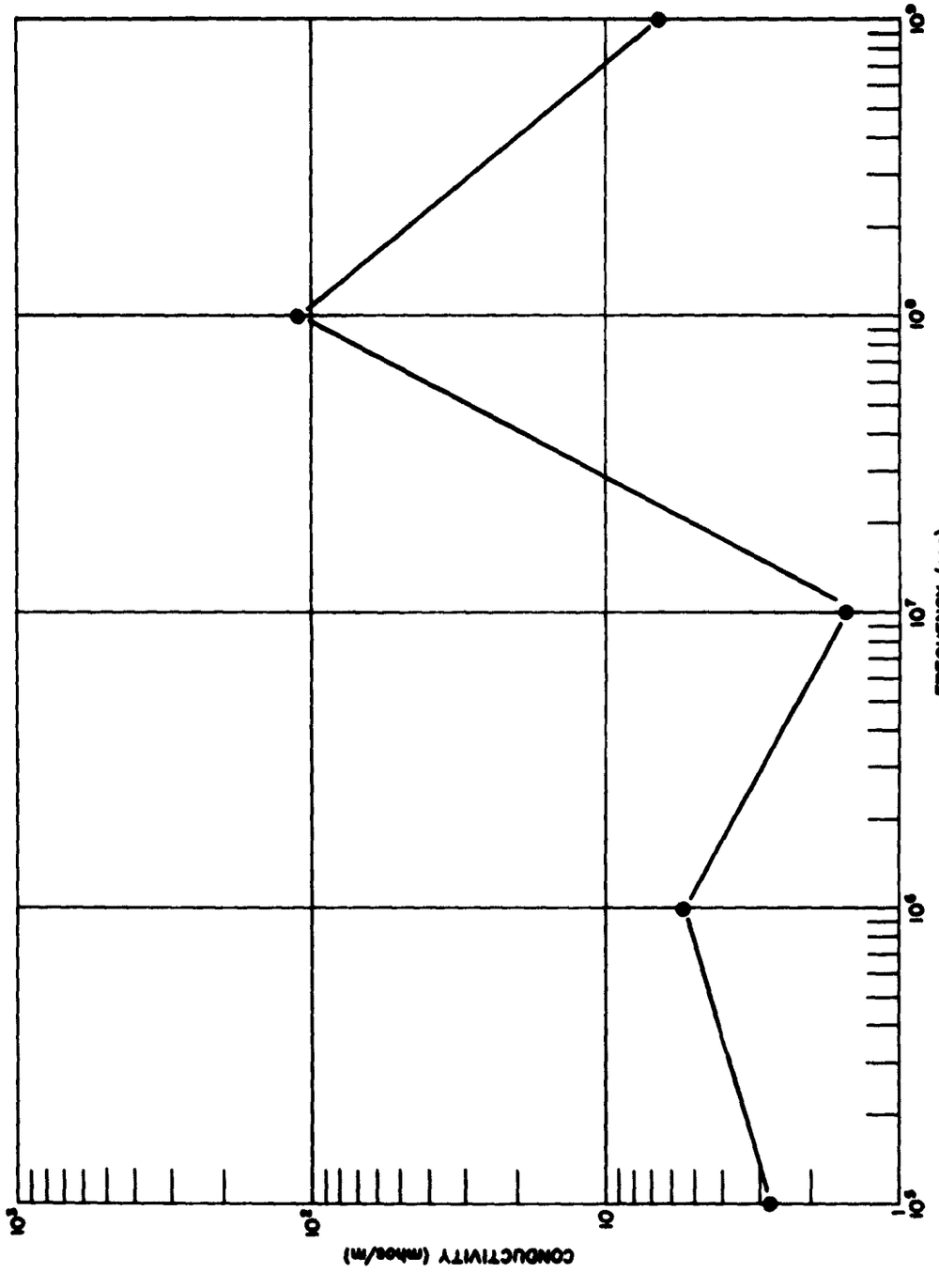

FIG. 2-6. CONDUCTIVITY VS. FREQUENCY FOR MODEL F

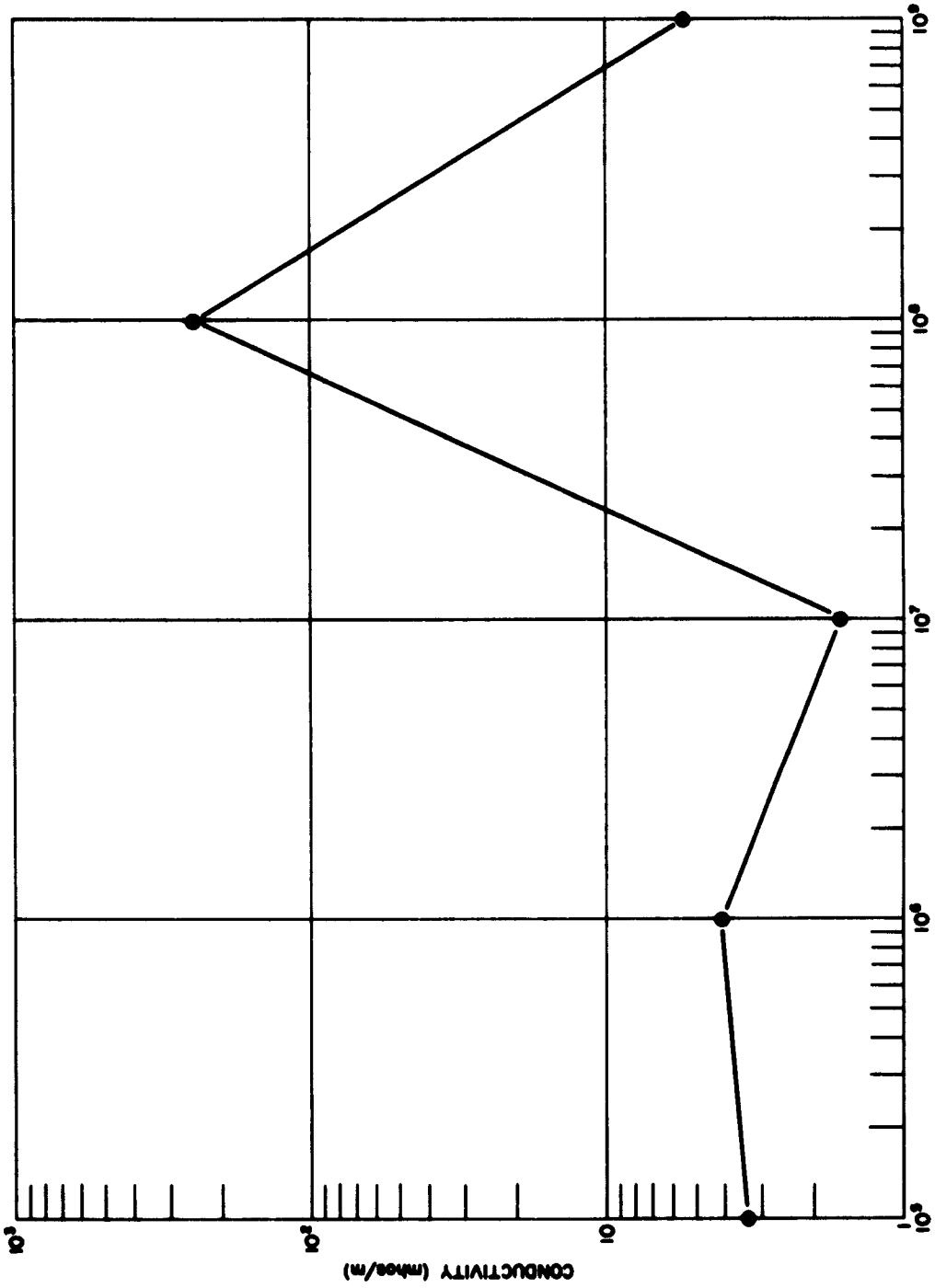

FIG. 2-7. CONDUCTIVITY VS. FREQUENCY FOR MODEL G

rearranging, the equation becomes:

$$\alpha = 128 \times 10^{-11} f \left[k'_\epsilon k'_\mu \left(\left(\frac{\epsilon''}{\epsilon'} \tan \delta_\mu - 1 \right) + \sqrt{\left(1 + \left(\frac{\epsilon''}{\epsilon'} \right)^2 \right) \left(1 + \tan^2 \delta_\mu \right)} \right) \right]^{\frac{1}{2}} \quad (2\text{-}2)$$

Substituting $\frac{\sigma}{2\pi f}$ for ϵ'', it can be shown that equation (2-2) takes the form

$$\alpha = 128 \times 10^{-11} f \left[k'_\epsilon k'_\mu \left(\left(\frac{\sigma \tan \delta_\mu}{2\pi f \epsilon'} - 1 \right) + \left(1 + \frac{\sigma^2}{4\pi^2 f^2 (\epsilon')^2} \right) \left(1 + \tan^2 \delta_\mu \right) \right) \right]^{\frac{1}{2}} \quad (2\text{-}3)$$

Analysis of equation 2-3 shows that an increase in σ (dielectric conductivity) should result in an increase of attenuation, if the other parameters are not adversely affected by this change.

2.1.2 Attenuation Measurements of Ferrites

In the course of our measurement program, we have had difficulty at times in the seating of samples in the holders. In an attempt to avoid the difficulty, we have silvered the outer and inner diameters of the toroids. We have observed that attenuation values are significantly increased. The values of the resistance have been measured and show a corresponding decrease.

We have tabulated in Table 2-1 the correlation between the lowering in resistance or, if you will, increase in conductivity when the toroids are silvered. It should be noted that the ratio of resistances before and after silvering and the ratio of attenuations before and after silvering are practically equal.

In order to eliminate the contribution, if any, of the silver in the conductive coating of Aquadag was used and the samples measured. Here again, an increase in attenuation was noted but to a lesser degree than when the sample is silvered.

It is possible that silvering increases the conductivity of the sample, thus increasing the lossy part of the permittivity (ϵ'') solely and has little or no effect on the other parameters.

Table 2-1

EFFECT OF SILVERING UPON ATTENUATION

Sample Number	R_B* (ohm)	R_A† (ohm)	R_B/R_A	α_B (db/cm) (500 Mc)	α_A (db/cm) (500 Mc)	α_B/α_A (500 Mc)
6425	1700	450	3.78	60	234	3.9
4498	4400	1200	3.67	24.2	115	4.75
4496	3000	793	3.79	24	92	3.8
6402	200	85	2.58	74.5	180	2.42
4499	3000	550	5.45	40	235	5.9
6397	140	38	3.68	42	82	2
6399	200	39	5.13	42	252	6

*R_B before silvering †R_A after silvering

We have measured several C27 toroids both silvered and unsilvered in our immittance bridge system. The data from these measurements will be processed in the computer and values of the various parameters calculated. We hope to determine if silvering does anything to the parameters.

2.2 Fabrication of Ferrites

Contributor: Lewis E. Katz

Importance of the ferrous ion content in ferrites, in relation to the conductivity and thus to attenuation, was discussed in the last report. It was noted that to obtain ferrous ions rather than ferric ions in the lattice structure it would be necessary to prevent contact with air (oxygen) during the decomposition of the oxalates and during the cooling following firing operation.

We have established a procedure whereby air is excluded during the decomposition of the oxalates. The oxalate is decomposed by heating it in a vessel closed with a two-hole rubber stopper. One hole is fitted with a stopcock, normally closed. The other hole provides connection, by means of glass and rubber tubing, through a water trap to a water filled flask. During heating of the vessel containing the oxalate, the gases which come off (CO and CO_2) pass through the tubing, through the water

trap and thence into the flask of water. Air is not permitted to enter the system during the decomposition. Following decomposition, the vessel which now contains ferrite, is cooled, drawing back the CO and CO_2 from the tubing and water trap. To replace the gases drawn from the water trap, water is drawn from the flask into the water trap where it is trapped. Thus, during cooling no air is allowed to enter the system. Before admitting air it is necessary to insert enough benzene through the stopcock to wet the ferrite, thus making certain that there is no oxidation upon contact with the air. The benzene is subsequently evaporated from the ferrite under a hood.

If we wish to preserve the ferrous ions present during firing, the material must be cooled very rapidly. Furnace cooling is extremely slow and allows enough time for the ferrous ions to oxidize to ferric ions. Air cooling is reasonably rapid and does not set up the severe thermal stresses caused by water quenching. Samples which are subjected to water quenching tend to crack easily due to the stress set up by the rapid cooling. It may be possible to obtain samples which do not crack during quenching by using a medium having a lower thermal conductivity than water at room temperature such as oil or hot water.

A large number of samples were prepared, having various compositions, using different pressures and firing temperatures, and cooling them at different rates (furnace cooling, air cooling, water quenching). These samples are tabulated in Table 2-2.

It is immediately evident from the table that those samples which were furnace cooled had very high resistance and low attenuation in comparison with those samples which were air cooled or water quenched. The low resistance of the latter compares favorably with C-27 and T-1 ferrites. As can be seen, silvering the samples results in lower resistance and higher attenuation. The effect of silvering the edges of ferrite samples is discussed in Section 2.1.2 of this report.

Table 2-2

FIL MADE FERRITES

Sample No.	Composition	Pressure (psi)	Firing Temperature (°C)	Cooling	Density (gm/cm³)	Resistance (ohms)	Attenuation (db/cm)
6774	$Ni_{0.5}Zn_{0.5}Fe_2O_4$	60,000	1300	air	4.02	1600	10.2 at 500 Mc
6775	$Ni_{0.5}Zn_{0.5}Fe_2O_4$	60,000	1300	air	4.22	850	14.7 at 500 Mc
6776	$Ni_{0.5}Zn_{0.5}Fe_2O_4$	85,000	1300	air	4.46	650	17.5 at 500 Mc
						150	36.8* at 500 Mc
							21.2* at 400 Mc
							16.6* at 300 Mc
							12.7* at 200 Mc
6777	$Mn_{.67}Zn_{.33}Fe_2O_4$	85,000	1300	air	3.80	cracked during grinding	
6778	$Ni_{0.5}Zn_{0.5}Fe_2O_4$	85,000	1315	furnace	4.22	120,000	3.15 at 500 Mc
6779	$Ni_{0.5}Zn_{0.5}Fe_2O_4$	85,000	1315	water	4.29	cracked	
6780	$Mn_{0.67}Zn_{0.33}Fe_2O_4$	85,000	1315	furnace	3.79	8,000,000	2.73 at 500 Mc
6781	$Mn_{0.67}Zn_{0.33}Fe_2O_4$	85,000	1315	water	3.72	cracked	
6788	$Ni_{0.5}Zn_{0.5}Fe_2O_4$	85,000	1325	furnace	4.43	500,000	3.36 at 500 Mc
6789	$Ni_{0.5}Zn_{0.5}Fe_2O_4$	85,000	1325	air	4.45	1000	22.1 at 500 Mc
							32.9* at 500 Mc
							26.5* at 400 Mc
							22.1* at 300 Mc
							20.8* at 200 Mc
6790	$Ni_{0.64}Zn_{0.36}Fe_2O_4$	85,000	1325	furnace	4.38	240,000	2.38 at 500 Mc
6791	$Ni_{0.64}Zn_{0.36}Fe_2O_4$	85,000	1325	air	4.36	340	15.5 at 500 Mc
6792	$Ni_{0.5}Zn_{0.5}Fe_2O_4$	60,000	1325	H_2O	3.95	cracked	
6793	$Ni_{0.64}Zn_{0.36}Fe_2O_4$	85,000	1325	furnace	4.50	400,000	5.1 at 500 Mc
6794	$Ni_{0.64}Zn_{0.36}Fe_2O_4$	85,000	1325	air	4.52	1000Ω	19.8 at 500 Mc
						65*Ω	38.4* at 500 Mc
							34.4 at 400 Mc
							25.8 at 300 Mc
							22.4 at 200 Mc
6795	$Ni_{0.64}Zn_{0.36}Fe_2O_4$	60,000	1325	water	4.10	180Ω	29.0 at 500 Mc
6796	$Ni_{0.64}Zn_{0.36}Fe_2O_4$	60,000	1325	air	4.27	cracked	

*silvered edges

Furthermore, we have succeeded in increasing the density of the nickel-zinc ferrites to such a value that they are comparable to the commercial ferrites. We attribute the increase in density to the higher firing temperatures which were used. The manganese-zinc samples produced by our procedure do not yet have satisfactory density, and this problem will have to be resolved. It is felt that emphasis should be placed on the Ni-Zn system due to the encouraging results obtained.

There appears to be no significant difference in the $Ni_{0.5}Zn_{0.5}Fe_2O_4$ and $Ni_{0.64}Zn_{0.36}Fe_2O_4$ ferrites in respect to their ability to attenuate. Primary consideration appears to be the ferrous ion content (as shown by low resistance), established during firing. Treatment of the samples with benzene during the decomposition of the oxalates appears to be less important, since those samples that were furnace cooled after firing had low attenuation in spite of benzene treatment.

Samples No. 6776, 6789, 6794 with high attenuation at 500 Mc, were silvered and measured at 200, 300, 400 and 500 Mc. Samples No. 6789 and No. 6794 measured over 20 db/cm at 200 Mc.

Sample No. 6795 is particularly interesting since it was the only water quenched sample which had enough strength to be ground and measured. Unfortunately, it did break before it could be silvered and evaluated at the various frequencies. This one showed the lowest resistance and highest attenuation (29.0 db/cm at 500 Mc) of any of those listed in Table 2-2, when unsilvered. This was expected since it was subjected to the most rapid cooling and should therefore contain the greatest number of ferrous ions. As noted previously, attempts will be made to quench additional samples in either hot water or oil.

Since control of oxygen during cooling appears to be so important, we are preparing a set-up which will allow firing and cooling in an inert atmosphere. Such a system should be very effective in preserving the ferrous ions.

2.3 Effect of Ferrite Attenuators on Firing Stimuli

In our search for an RF attenuating material, we have not lost sight of the fact that the EED being protected does have to be initiated by some type of firing pulse. During November, we conducted two experiments to determine the effect of a ferrite attenuator on capacitor discharge and constant current pulses.

2.3.1 Capacitor Discharge

A block diagram of the system for determining the effect of a ferrite sample on a capacitor discharge pulse is shown in Figure 2-8. Capacitor C is charged to voltage E and then discharged into load R_L by switch S. A dual channel oscilloscope records the pulse at the input

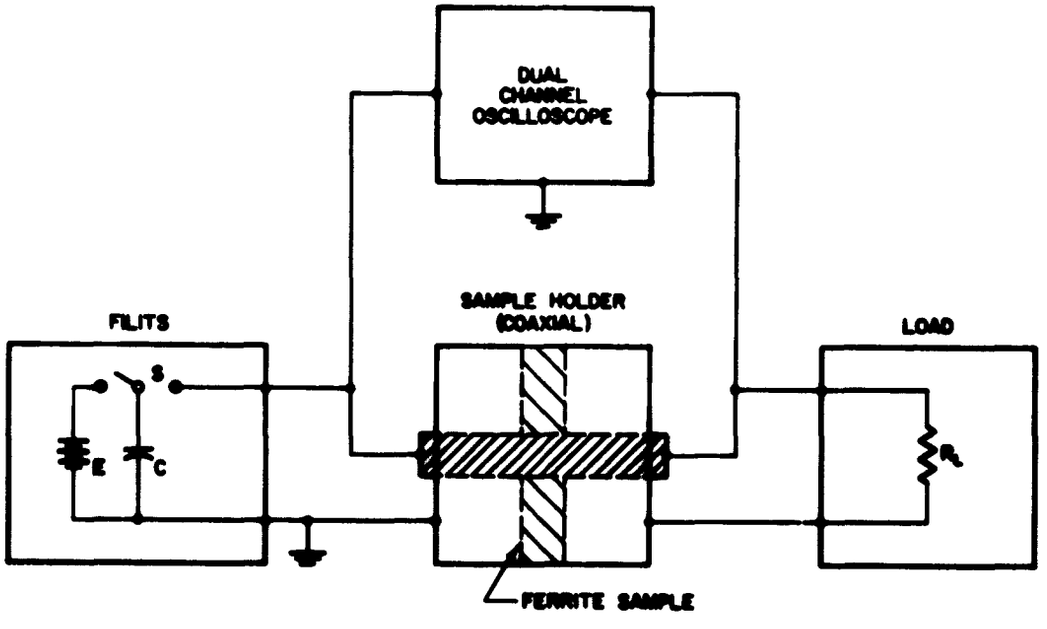

FIG. 2-8. CAPACITOR DISCHARGE EVALUATION EQUIPMENT

side of the sample holder and at the load. The oscillograms in Figure 2-9 indicate that the ferrite attenuators have a negligible effect on capacitor discharge pulses.

Several other experiments were conducted in which the value of the capacitor was decreased from 1.0 μf to 0.001μf. Even when a one-ohm load was used, no adverse effect on the pulse was noted.

2.3.2 Constant Current

The same general setup, shown in Figure 2-8, was used for constant current evaluation except that the capacitor discharge unit was replaced by a constant current generator. The effect upon a five-ampere pulse applied to a one-ohm load is shown in Figure 2-10. Once again, no detriment was noted.

2.4 Material Evaluation - Organic Materials

Contributor: Ernst R. Schneck

We have over the past few years investigated various materials that could possibly absorb undesired electromagnetic energy and thereby prevent its passage into an electroexplosive device. In recent years, interest and studies in organic semiconductors has increased considerably, and consequently we have sought to determine the state of the art regarding RF absorption in organics, to aid in evaluating the probability of practical applications.

Organics, in general, differ from inorganics (such as ferrous compounds) by the lack of ferromagnetic properties. Inclusion of ferrous materials in the organic substance will impart an increased permeability and ferromagnetic activity[1]. In general, however, only permittivity is considered when describing losses in organics. Generally, organics possess permittivities well below those of certain inorganics (such as ferrites) and, correspondingly, have low dielectric loss tangents.

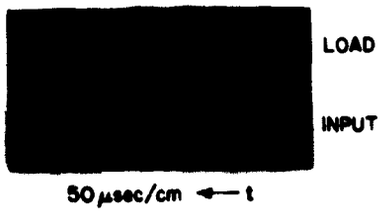

(a) 1μf - 50 ohm Load

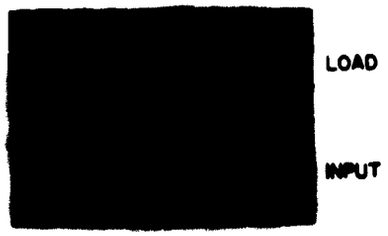

(b) 1μf - 1 ohm Load

FIG. 2-9. CAPACITOR DISCHARGE PULSES

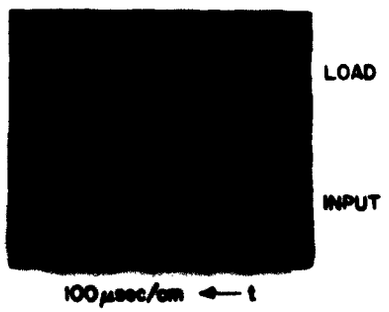

FIG. 2-10. CONSTANT CURRENT PULSES
(1 ohm Load)

However, organic dielectric loss tangents greater than one are known[2]. Organic polymers form the molecular type to which most lossy organics belong.

Polymeric materials may be divided into two main classes; polar, which have permanent dipoles, and non-polar, which do not[3]. The dipoles are formed by opposite pairs of charges which are separated by some finite distance, and alignment with an impressed field is the mechanism through which energy is dissipated. Polar polymers are characterized chiefly by asymmetrical molecular arrangements, and may possess significant loss tangents[4].

Certain physical relations of permittivity complicate dielectric absorption phenomena in organics. Among the most important are temperature dependence[2], and variation among different crystalline axes[5]. The extent to which these may be easily controlled is not yet apparent.

Conclusions regarding the prospective usefulness of organic materials to absorb RF are not yet possible; we shall continue our investigation toward this end.

3. APPLIED STUDIES

3.1 Dielectric Insulators

Contributor: James D. Dunfee

High-K dielectric insulating films, when applied to initiator conductors, can increase the voltage breakdown and insulation resistance of the attenuating assembly. Research has indicated that the insulation thickness and the material dielectric constant must be carefully specified to maintain the attenuation of the insulated assembly close to that attained by the uninsulated configuration. Attempts to sinter barium titanate in position on a metallic conductor have not been successful. Unfortunately, $BaTiO_3$ appears to realize a dielectric constant in the range of K = 1500 only in the fired ceramic form. We are presently evaluating an insulating coating composed of a matrix of pre-heat treated $BaTiO_3$ in an acryloid

binder. Dielectric constants above 50 do not appear feasible using such a mixture. However, three mil coatings of this high dielectric strength insulation may be useful in practical applications.

3.1.1 Preparation of High-K Dielectric Coatings

During this report period, we continued evaluating the $BaTiO_3$ coatings with acryloid binder. The Mixture evaluated is as follows:

		After Xylene Evaporation	
Orig. Mixture	Percent by Wt.	Percent by Wt.	Percent by Vol.
$BaTiO_3$	60.8%	85.5%	55.3%
Bentone 38	1.3%	1.8%	3.6%
Xylene	28.8%	EVAP	EVAP
Acryloid B-72	9.1%	12.8%	41.1%

For dipped coatings averaging 3 mils thick on stainless wire, the dielectric constant averaged 28.5. Using Lichtenecker's approximation* for dielectric constant of a mixture.

$$\text{Log (K of Mixt.)} = (\text{Vol. fract. binder})(\log K \text{ of a binder}) + (\text{Vol. fract. } BaTiO_3)(\log K \text{ of } BaTiO_3)$$

we find that the average K of $BaTiO_3$ in small particle (3 micron or less) non-ceramic polycrystalline form is 148. If we use this value in the equation for a higher concentration (90% by wt. $BaTiO_3$) of this mixture, a value of K = 40 for the insulating coat should be obtained. We have so far not been able to increase the K of the coating on the wire with such a mixture, as calculated. An analysis of the actual percentages of constituents of the coating may reveal the reason for the lack of success.

We have determined the attenuation losses for a three-mil coating of the mixture discussed previously. Results are shown in Table 3-1. Note that Sample No. 6784 has a considerably larger decrease in attenuation than the other samples, but no reasons for this could be found. Sample No. 6785 incorporated a new higher strength acryloid binder which will be used in all new formulations.

*Lichtenecker, K., and Rother, K., 1931, Phys. Z., 32, 255.

We plan to optimise the dielectric constant using this type coating and then test a sample group of sufficient size to determine expected decreases in attenuation for this insulating coating.

Table 3-1

FERRITES WITH DIELECTRIC COATING

Sample No.	Insulation	Attenuation db/cm at 500 Mc	% Loss for .003 thickness
6782	uncoated	30	———
6783	uncoated	27	———
	Aug	28.5	———
6784	$BaTiO_3$ - Acryloid B-72	19	33%
6785	$BaTiO_3$ - Acryloid B-44	23	19%
6786	$BaTiO_3$ - Acryloid B-72	24	16%
6787	$BaTiO_3$ - Acryloid B-72	24	16%

4. INSTRUMENTATION

4.1 Determination of Attenuation

Contributor: Charles L. Stonecypher

During November, an attempt was made to solve applicable equations to give maximum power transfer through a section of transmission line having a fixed propagation constant and a fixed characteristic impedance, by varying the reflection coefficient. The solution was expected to yield an explanation of the process which gives maximum transfer (minimum loss); however, the maximization was found to be involved, and no simple solution could be obtained. A parallel analysis that yields the conditions of the terminating impedance in terms of transmission line characteristic impedance and propagation constant was completed and is presented.

4.1.1 A Solution for the Terminating Impedance Corresponding to Minimum Loss for a Section of Transmission Line

Consider the terminated section of transmission line shown in Figure 4-1. The stated problem is the minimisation of the ratio of the power at A-A to that at B-B$\left(P_A/P_1\right)$ by varying the terminating impedance. If the transmission line is lossless, the minimum ratio is one. Under all other conditions the ratio is greater than one. The conditions imposed upon the terminating impedance for minimisation of the ratio are derived as follows.

The power P at A-A and B-B is written in terms of the voltage V and current I on the transmission line. The wave solutions for a distributed transmission line will not be derived since they are adequately treated in many texts. The time variance of the voltage and current functions is taken to be $Re(e^{j\omega t})$

$$V = \left[Ae^{-\gamma x} - Be^{\gamma x}\right] Z_o$$

$$I = Ae^{-\gamma x} + Be^{\gamma x}$$

$$P = VI^*$$

$*$ = complex conjugate

To compute power, I* must be known. A was arbitrarily taken to be a real number, but B is free to take on values in the Gaussian plane. Therefore, B was related to A, γ, and Z_R at the boundary B-B.

$$\frac{V_B}{I_B} = Z_R$$

Taking x to be 1 at B-B sacrifices nothing since the calibration of a linear scale is arbitrary.

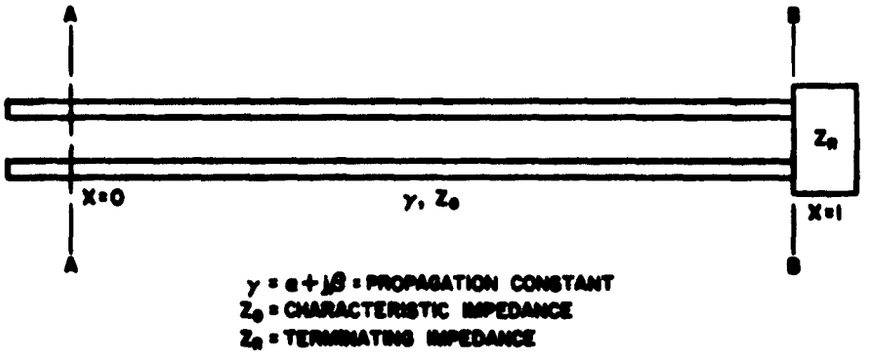

FIG. 4-1. A TERMINATED SECTION OF TRANSMISSION LINE

$$\frac{\left(Ae^{-\gamma} - Be^{\gamma}\right) Z_o}{Ae^{-\gamma} + Be^{\gamma}} = Z_R$$

$$B = Ae^{-2\gamma} \frac{Z_o - Z_R}{Z_o + Z_R}$$

The coordinate (x) at A-A was taken to be zero and the expression for power at A-A (P_A) and B-B (P_B) were written.

$$P_A = V_A I_A^* = Z_o (A-B)(A+B^*)$$

$$P_B = V_B I_B^* = Z_o (Ae^{-\gamma} - Be^{\gamma}) I_B^*$$

B^* and I^* were evaluated by writing Z_o and Z_R in polar form and making the appropriate substitutions.

$$Z_o = De^{j\phi} \qquad Z_R = Ce^{j\theta}$$

Reforming the expression for B:

$$B = \frac{Ae^{-2\alpha}}{Z_o + Z_R}\left[De^{j(\phi - 2\beta)} - Ce^{j(\theta - 2\beta)}\right]$$

$$B^* = \frac{Ae^{-2\alpha}}{\left(Z_o + Z_R\right)^*}\left[De^{-j(\phi - 2\beta)} - Ce^{-j(\theta - 2\beta)}\right]$$

$$I_B{}^* = \left(Ae^{-\gamma}\right)^* + \left(Be^{\gamma}\right)^* = \frac{2\,AD\,e^{-\alpha}}{\left(Z_o + Z_R\right)^*}\,e^{-j(\phi - \beta)}$$

Consider first the power at A-A.

$$P_A = V_A\,I_A{}^* = Z_o\,(A-B)(A+B^*)$$

$$= \frac{A^2D\left[e^{j\phi(\nu)} + e^{-2\alpha}\left(e^{j(2\beta + \phi)}\,\xi - e^{-j(2\beta - \phi)}\,\psi\right) - e^{-4\alpha + j\phi(\eta)}\right]}{\left(Z_o + Z_R\right)\left(Z_o + Z_R\right)^*}$$

$$\nu = D^2 + 2\,CD\cos(\theta - \phi) + C^2$$

$$\psi = D^2 - CD\left(e^{j(\theta - \phi)} - e^{-j(\theta - \phi)}\right) - C^2$$

$$\xi = D^2 + CD\left(e^{j(\theta - \phi)} - e^{-j(\theta - \phi)}\right) - C^2$$

$$\eta = D^2 - 2\,CD\cos(\theta - \phi) + C^2$$

In taking the real part of this apparent power expression the first and last term coefficients (ν, η) go unchanged. Some manipulation of the intermediate term was necessary.

$$\underline{\text{Re}}\ (P_A) = P_o = \frac{DA^2}{\left(Z_o + Z_R\right)\left(Z_o + Z_R\right)^*}\left[\cos\phi\ (\nu) - 2e^{-2\alpha}\sin\phi\ (\Omega) - e^{-4\alpha}\cos\phi\ (\eta)\right]$$

$$\Omega = 2CD\cos 2\beta\sin(\theta-\phi) + \sin 2\beta\left(D^2 - C^2\right)$$

Now consider the power at B.

$$P_B = V_B\, I_B^*$$

$$= \left(\frac{2ACD\,e^{-\alpha}}{Z_o + Z_R}\right)e^{j(\theta+\phi-\beta)}\left(\frac{2AD\,e^{-\alpha}}{\left(Z_o + Z_R\right)^*}\right)e^{-j(\phi-\beta)}$$

V_B was formed by substituting B and Z_o in the polar form into the fundamental voltage expression evaluated at x = 1.

$$\underline{\text{Re}}\ (P_B) = P_1 = \frac{4A^2D^2C\,e^{-2\alpha}}{\left(Z_o + Z_R\right)\left(Z_o + Z_R\right)^*}\cos\theta$$

The ratio $\left(P_o/P_1\right)$ can now be written.

$$\frac{P_o}{P_1} = \frac{\cos\phi\ (\nu) - 2e^{-2\alpha}\sin\phi\ (\Omega) - e^{-4\alpha}\cos\phi\ (\eta)}{4Ce^{-2\alpha}\cos\theta}$$

The conditions on the terminating impedance magnitude (c) and the phase angle (θ) to minimize the ratio $\left(P_o/P_1\right)$ were obtained by setting $\frac{\partial\left(\frac{P_o}{P_1}\right)}{\partial c}$ and $\frac{\partial\left(\frac{P_o}{P_1}\right)}{\partial\theta}$ equal to zero. The minimization with respect to c led to the following condition:

$$C = D\left[\frac{1 - 2\,e^{-2\alpha}\tan\phi\sin 2\beta - e^{-4\alpha}}{1 + 2\,e^{-2\alpha}\tan\phi\sin 2\beta - e^{-4\alpha}}\right]^{\frac{1}{2}}$$

$$\theta \neq n\frac{\pi}{2} \qquad n = 1, 3, 5, 7, \ldots\ldots$$

The minimization with respect to θ, led to the condition:

$$\sin\theta = \frac{(-2DC\sin\phi)\left[1 - 2\,e^{-2\alpha}\cos 2\beta + e^{-4\alpha}\right]}{(C^2 + D^2) - 2\,e^{-2\alpha}\tan\phi\sin 2\beta\,(D^2 - C^2) - e^{-4\alpha}\,(D^2 + C^2)}$$

Substitution for c reduces the expression.

$$\sin\theta = \sin(-\phi)\,\frac{1 + e^{-4\alpha} - 2\,e^{-2\alpha}\cos 2\beta}{\left[\left(1 - e^{-4\alpha}\right)^2 - \left(2\,e^{-2\alpha}\tan\phi\sin 2\beta\right)^2\right]^{\frac{1}{2}}}$$

Clearly, the measurement of open and short circuit impedances on a symmetrical section of transmission line defines γ and Z_o. Thus, these results can be used to yield the minimum $\frac{P_o}{P_l}$ and correspondingly a minimum loss for a section of symmetrical transmission line.

Upon completion of the substitutions for the load impedance magnitude and phase angle into the power ratio expression a minimum loss condition will be established in terms of γ or Z_o for a section of transmission line (sample). It is hoped that the analysis will yield a clearer picture of the conditions causing minimum loss and open an avenue through which further optimization of attenuating material properties can be made.

5. CONCLUSIONS AND FUTURE PLANS

Ferrites

Computer data from the immittance bridge measurements on silvered and unsilvered toroids should be completed and comparison made of the changes in any or all of the parameters. A report will be made of the effect of gaps between the outer periphery of toroids and the inner surface of the outer conductor for both silvered and unsilvered samples.

Specially fired T-1 ferrite toroids have still to be evaluated. Difficulties in mounting these samples should be resolved in the coming period and it is expected that we will be able to report data for these samples.

It is possible to make high loss Ni-Zn ferrites by maintaining ferrous ions in the lattice. This is accomplished by rapidly cooling the fired body, allowing little time for the ferrous ions to oxidize to ferric ions. Attempts will be made to cool the fired bodies in substances other than air and cold water. We plan to fire and cool a group of samples at higher temperatures than presently used in an effort to increase their density.

Results of the study on firing pulses passing through a ferrite attenuator were encouraging. Because the ferrite does not alter a transient-type stimulus, the material can be used in most types of EED's. One exception to this may be the EBW which requires 2000 volts. Under such an electrical stress, the ferrite may break down. We have not yet investigated this characteristic of the ferrites.

Organic Materials

The use of organic materials as RF attenuators is an interesting possibility. Our main reason for considering this class of materials is the large loss tangents that are cited in the literature. Values as high as 1.7 can be obtained. Whether these values can be realized in a practical material will have to be determined. Obviously, if they are

available, say only in liquid form, it is almost certain that they could not be put to practical use.

Dielectric Insulators

Using our acryloid-bound barium titanate insulating coat on wires, an attenuation loss of 20% or less with a voltage breakdown of 500-600 volts for a 3-mil coating is expected.

While the dielectric constant of $BaTiO_3$ in the fully fired ceramic form is approximately K = 1500 at room temperature, values for the dielectric constant of the powdered $BaTiO_3$ appear to range from 100 to 200. Little if any information is available in this regard for $BaTiO_3$ and most other materials which are ordinarily utilized in the fully fired densified polycrystalline ceramic form. We plan to test a number of other insulating materials which may have a high dielectric constant in powdered form, such as titanium dioxide and prefired ferrites.

Instrumentation

During December, the analysis presented in this report will be continued and a series of measurements made on ferrite samples by the "matched" system and the $\bar{A}$ parameter system. Impedance measurements that yield "worst-case" loss values will be made and evaluated by the computer program previously written for this task. Additionally, a program will be written for the evaluation of "worst-case" attenuation for a non-symmetrical network. When this program is completed and checked out, we shall be equipped to measure "worst-case" attenuation for both symmetrical and non-symmetrical networks.

Paul F. Mohrbach
Project Leader

Robert F. Wood
Project Engineer

Approved by:

E. B. Hanmum
Applied Physics Laboratory

Francis L. Jackson
Director of Laboratories

BIBLIOGRAPHY

1. Y. G. Dorfman; Concerning the Nature of the Unusual Magnetic Phenomena Exhibited by Certain Organic Materials, Dokl. Akad. Nank SSR, 142, 815, #4, 1962.

2. A. Lurio, E. Stern; Dielectric Behavior of Single Crystals of Triglycine Sulfate from 1 Kc to 2500 Mc, J. Appl. Phys. 31, 1125, June 1960.

3. Birks and Schulman; Progress in Dielectrics, Vol. II, J. Wiley & Sons, 1960.

4. N. P. Bogoroditski and V. V. Pasynkov; Materials in Radio Electronics ASTIA #AD-275 736 (Chapter 3).

5. E. Rushton; Dielectric Properties of Ammonium Dihydrogen Phosphate at Very High Frequencies, Brit. J. Appl. Phys. 12, 417, August 1961.

P-B1981-5

DISTRIBUTION LIST

U.S. Naval Weapons Laboratory
Dahlgren, Virginia
Attn: Code WHR (2)

Chief, Naval Operations (OP-411H)
Department of the Navy
Washington 25, D. C.

Chief, Bureau of Naval Weapons
Department of the Navy
Washington 25, D. C.
Attn: Code C-132
Code RAAV-3421
Code RM-15
Code RMMO-224
Code RMMO-235
Code RMMO-32
Code RMMO-33
Code RMMO-4
Code RMMO-43
Code RMMO-44
Code RMMP-343
Code RREN-312
Code DIS-313 (4)

Chief, Bureau of Medicine and Surgery
Department of the Navy
Washington 25, D. C.
Attn: Code 74

Chief, Bureau of Yards and Docks
Department of the Navy
Washington 25, D. C.
Code D-200

Commander
U.S. Naval Ordnance Laboratory
White Oak, Maryland
Attn: Code ED
Code NO
Code LV
Code Technical Library

Commander
U.S. Naval Ordnance Laboratory
Corona, California
Attn: Code 561
Code 552

Commander
U.S. Naval Ordnance Test Station
China Lake, California
Attn: Code 556
Code 4572

Commanding Officer
U.S. Naval Air Development Center
Johnsville, Pennsylvania
Attn: Code EL-94

Commanding Officer
U.S. Naval Underwater Ordnance Station
Newport, Rhode Island

Director
U.S. Naval Research Laboratory
Washington 25, D. C.
Attn: Code 5439
Code 5410 (2)

Commanding Officer
U.S. Naval Nuclear Ordnance Evaluation Unit
Kirtland Air Force Base
Albuquerque, New Mexico
Attn: Code 40

Commandant of the Marine Corps
Washington 25, D. C.
Attn: Code AO4C

Commander
Pacific Missile Range
P.O. Box 8
Point Mugu, California
Attn: Code 3260

P-B1981-5

DISTRIBUTION LIST

Commanding Officer and Director
U.S. Navy Electronics Laboratory
San Diego 52, California
Attn: Code Library

Commanding Officer
U.S. Naval Ordnance Plant
Macon, Georgia
Attn: Code PD 270

Commander Naval Air Force
U.S. Atlantic Fleet CNAL 724B
U.S. Naval Air Station
Norfolk 11, Virginia

Commander Service Force
U.S. Atlantic Fleet
Building 142, Naval Base
Norfolk 11, Virginia

Commander Training Command
U.S. Pacific Fleet
c/o U.S. Fleet Anti-Submarine
Warfare School
San Diego 47, California

Commanding General
Headquarters, Fleet Marine Force,
Pacific
c/o Fleet Post Office
San Francisco, California
Attn: Force Communications
Electronic Officer

Commander in Chief
U.S. Pacific Fleet
c/o Fleet Post Office
San Francisco, California
Attn: Code 4

Commander Seventh Fleet
c/o Fleet Post Office
San Francisco, California

Commander
New York Naval Shipyard
Weapons Division
Naval Base
Brooklyn 1, New York
Attn: Code 290
Attn: Code 912B

Commander
Philadelphia Naval Shipyard
Naval Base
Philadelphia 12, Pennsylvania
Attn: Code 273

Commander
Pearl Harbor Naval Shipyard
Navy No. 128, Fleet Post Office
San Francisco, California
Attn: Code 280

Commander
Portsmouth Naval Shipyard
Portsmouth, New Hampshire

Department of the Army
Office Chief of Ordnance
Washington 25, D. C.
Attn: Code ORDGU-SA
Code ORDTN
Code ORDTB (Research &
Special Projects)

Office Chief Signal Officer
Research and Development Division
Washington 25, D. C.
Attn: Code SIGRD-8

Commanding Officer
Diamond Ordnance Fuse Laboratories
Washington 25, D. C.
Attn: Mr. T. B. Godfrey

P-B1981-5

DISTRIBUTION LIST

U.S. Army Nuclear Weapon Coordination Group
Fort Belvoir, Virginia

Director
U.S. Army Engineer Research and Development Labs.
Fort Belvoir, Virginia
Attn: Chief, Basic Research Group

Commanding Officer
Picatinny Arsenal
Dover, New Jersey
Attn: Artillery Ammunition & Rocket Development Laboratory
Mr. S. M. Adelman

Commanding Officer
U.S. Army Environmental Health Lab.
Building 1235
Army Chemical Center, Maryland

Commanding General
Headquarters 2DRAADCOM
Oklahoma City, AFS
Oklahoma City, Oklahoma

Commanding Officer
U.S. Army Signal Research & Development Laboratory
Fort Monmouth, New Jersey
Attn: SIGEM/EL-GF

Commander
U.S. Army Rocket and Guided Missile Agency
Redstone Arsenal, Alabama
Attn: ORDXR-R (Plans)

Commanding Officer
Office of Ordnance Research, U.S. Army
Box CM, Duke Station
Durham, North Carolina
Attn: Internal Research Division

Commanding General
White Sands Missile Range
New Mexico
Attn: Code ORDBS-G3

Commanding Officer
White Sands Missile Range,
New Mexico
U.S.A. SMSA
Attn: Code SIGWS-AJ (4)

Commanding General
U.S. Army Electronic Proving Ground
Ft. Huachuca, Arizona
Attn: Technical Library

Director of Office of Special Weapons Development
United States Continental Army Command
Fort Bliss, Texas
Attn: Capt. Chester I. Peterson
T S Control Officer

Headquarters
Air Research & Development Command
Andrews Air Force Base
Washington 25, D. C.
Attn: Code RDRMS-3

Commander
Air Force Missile Test Center
Patrick Air Force Base, Florida
Attn: Code MTRCF

Headquarters
Ogden Air Material Area
Hill Air Force Base
Ogden, Utah
Attn: Code OOYSS

Commander, Charleston Naval Shipyard
U.S. Naval Base
Charleston, South Carolina

P-B1981-5

DISTRIBUTION LIST

Griffiss Air Force Base
RADC New York
Attn: RCLS/Philip L. Sandler

Commander
Air Force Special Weapons Center
Kirtland Air Force Base
Albuquerque, New Mexico
Attn: Code SWVSA

Commanding General
Air Fleet Marine Force, Pacific
MCAS, El Toro
Santa Ana, California

Commander
Headquarters Ground Electronics
Engineering Installation Agency
Griffiss Air Force Base
Rome, New York
Attn: Code ROZMWT

Armed Services Explosives Safety Board
Department of Defense
Room 2075, Bldg. T-7, Gravelly Point
Washington 25, D. C.

Headquarters
Armed Services Technical Information
Agency
Arlington Hall Station
Arlington 12, Virginia
Attn: TIPCR (10)

Commander
Field Command
Defense Atomic Support Agency
Albuquerque, New Mexico
Attn: Code FCDR3

Defense Research Staff
Brittish Embassy
3100 Massachusetts Ave., N.W.
Washington 8, D. C.
Attn: Mr. G. R. Nice
VIA: Chief, Bureau of Naval Weapons
Department of the Navy
Washington 25, D. C.
Attn: Code DSC-3

Aerojet-General Corporation
P.O. Box 1947
Sacramento, California
Attn: R. W. Froelich, Dept. 6620
POLARIS Program

American Machine and Foundry Co.
Alexandria Division
1025 North Royal Street
Alexandria, Virginia
Attn: Dr. L. F. Dytrt
(Contr. AF-29(601)-2769)

Atlas Powder Company
Reynolds Ordnance Section
P.O. Box 271
Tamaqua, Pennsylvania
Attn: Mr. R. McGirr

The Bendix Corp.
Scintilla Division
Sidney, N. Y.
Attn: R. M. Purdy

Bermite Powder Company
22116 West Soledad Canyon Road
Saugus, California
Attn: Mr. L. LoFiego

Bethlehem Steel Company, CTD
97 E. Howard Street
Quincy, Massachusetts
Attn: Mr. W. C. Reid

Chance Vaught Corp.
P.O. Box 5907
Dallas 22, Texas
Attn: R. D. Henry

The Franklin Institute
20th & Benj. Franklin Parkway
Philadelphia 3, Pennsylvania
Attn: Mr. E. E. Hannum, Head
Applied Physics Lab.

P-B1981-5

DISTRIBUTION LIST

Grumman Aircraft Engineering Corporation
Weapons Systems Department
Bethpage, Long Island, New York
Attn: Mr. E. J. Bonah

Jansky and Bailey, Inc.
1339 Wisconsin Avenue, N.W.
Washington, D. C.
Attn: Mr. F. T. Mitchell, Jr.
(Contract N178-7604)

Librascope Division
General Precision, Inc.
670 Arques Avenue
Sunnyvale, California
Attn: Mr. R. Carroll Maninger

Lockheed Aircraft Corporation
P.O. Box 504
Sunnyvale, California
Attn: Missile Systems Division,
Dept. 62-20
Mr. I. B. Gluckman
Attn: Missiles and Space Division
Dept. 81-62
Mr. E. W. Tice
Attn: Missiles and Space Division
Dept. 81-71
Mr. R. A. Fuhrman

McCormick Selph Associates
Hollister, California
Attn: Technical Librarian

Midwest Research Institute
425 Volker Boulevard
Kansas City, Missouri
Attn: Security Officer
Mr. C. M. Fisher

RCA Service Company
Systems Engineering Facility
Government Service Department
838 N. Henry Street
Alexandria, Virginia

Sandia Corporation (Division 1262)
Albuquerque, New Mexico
Via: FCDASA

University of Denver
Denver Research Institute
Denver 10, Colorado
Attn: Mr. R. B. Feagin

U.S. Flare Division Atlantic
Research Corporation
19701 W. Goodvale Road
Saugus, California
Attn: Mr. N. C. Eckert, Head
R&D Group

Aerojet-General Corporation
P.O. Box 296
Azusa, California
Attn: M. Z. Grenier, Librarian

Welex Electronics Corporation
Solar Building, Suite 201
16th and K Streets, N. W.
Washington 5, D. C.

North American Aviation, Inc.
Communications Services
4300 East 5th Avenue
Col. 16, Ohio

Commander
U.S. Army Ordnance
Frankford Arsenal
Philadelphia 37, Pennsylvania

U.S. Atomic Energy Commission
Division of Military Application
Washington 25, D. C.

U.S. Naval Explosive
Ordnance Disposal Facility
U.S. Naval Propellant Plant
Indian Head, Maryland

P-B1981-5

DISTRIBUTION LIST

The Martin Company
P.O. Box 5837
Orlando, Florida
Attn: Engineering Library

Commanding Officer
Picatinny Arsenal
Dover, New Jersey
Attn: SMUPA-VP3
Plastics Technical Evaluation Center
A. M. Anzalone (2)